

# Integrated $2 \times 2$ Thermo-optic Silicon Oxynitride Optical Waveguide Switch Based on the Multimode Interference Effect

Ricky W. Chuang\* and Z. L. Liao

Associate Professor of Institute of Microelectronics, College of Electrical Engineering and Computer Science, National Cheng Kung University

rwchuang@mail.ncku.edu.tw

Journal of The Electrochemical Society, 2010, Vol. 157(2), H149-H152

The effect of multimode interference (MMI) have been utilized quite frequently to fabricate a variety of interesting integrated waveguide devices including  $N \times N$  power splitters/combiners [1], switches based on Mach-Zehnder interferometers (MZIs) [2], optical multiplexers/demultiplexers [3], and ring lasers [4]. What make these MMI-based devices so popular obviously are due to their relatively simple structures, large optical bandwidths, relatively low excess losses, and very little dependence in polarization. For the conventional  $2 \times 2$  MZI- and MMI-based optical switches, their overall lengths are usually kept very long in order to accommodate with a fact that their output waveguides are needed to be placed sufficiently far apart from each other in order to minimize the optical and electrical parasitical couplings. Therefore, reducing the length of a switching device while not adding unnecessary burden to its fabrication process become a top priority for realizing an optimal optical switch with much reduced footprint and low propagation and scattering losses. With the foregoing comment in mind, as shown in Fig. 1, our design is based on the integration of the four  $1 \times 1$  general MMI waveguides (or MMIs in short, with two being placed at each input and output terminal of an optical switch) with one  $2 \times 2$  paired MMI; our goal is to produce a multistage MMI-based optical switch with high extinction coefficient and low propagation and scattering losses.



The schematic drawings showing the device structure and its cross-sectional profile of the multimode waveguide with SiON core buried in SiO<sub>2</sub> layers sliced along the AA' line (not drawn to scale) are depicted in Fig. 1. The entire  $2 \times 2$  optical switch consists of multiple stages of MMI waveguides being integrated together, that is, with two general MMIs ( $W_{\text{Gen}} = 51 \mu\text{m}$  and  $L_{\text{Gen}} = 11030 \mu\text{m}$ ) at each input and output terminal of a  $2 \times 2$  paired MMI ( $W_{\text{Paired}} = 102 \mu\text{m}$  and  $L_{\text{Paired}} = 6960 \mu\text{m}$ ) at the middle section of the device. The widths of input/output waveguides and the connection waveguides between the general and paired MMIs are set at 10 and 12  $\mu\text{m}$ , respectively, in order to compensate in advance the possible width losses due to subsequent photolithography and inductively-coupled plasma (ICP) dry etching. The dimensions of these MMI waveguides are chosen in order to reflect a fact that the sum of ( $L_{\text{Gen}} + L_{\text{Paired}}$ ) is still comparably shorter than the length of  $2 \times 2$  general MMI waveguide, provided that the spacing ( $T$ ) between the two input or two output waveguides is still maintained at 116  $\mu\text{m}$ . Notice that the waveguide spacing  $T$  is purposely set to be a rather large value in order to minimize the possible crosstalk between the output waveguides while refraining from the use of S-bends for their inevitable propagation and scattering losses.

Before we proceeded on fabricating and characterizing the foregoing device, the entire  $2 \times 2$  MMI switch is simulated beforehand in order to verify its intended optical signal switch between the bar and cross output ports using the finite-difference beam propagation method (FD-BPM). The resultant FD-BPM simulation data shown as the normalized output powers of bar and cross terminals versus the applied heater temperature are depicted in Fig.

2. Accordingly, the first cross-over point corresponding to the initiation of light switch from bar to cross port occurs at 12 ° C, while the second cross-over point for light output going from cross to bar port begins to take place at around 33 ° C. Therefore, the resultant FD-BPM simulation unequivocally verified our integrated MMI switch has indeed served its design purpose.

As also shown in Fig. 1, when designing the multistage  $2 \times 2$  tunable MMI-based optical switch, both the multimode section and access (input/output) waveguides were fabricated using the SiO<sub>2</sub>/SiON/SiO<sub>2</sub> symmetrical waveguide layers structure. All of these dielectric layers were deposited in sequence on the silicon substrate with a thermal conductivity of  $\sim 140$  W/(m•K) using the plasma-enhanced chemical vapor deposition (PECVD) reactor. Initially, 3-  $\mu$  m-thick SiO<sub>2</sub> and 2.5-  $\mu$  m-thick SiON layers were deposited first on silicon. Next, input, output, and multimode waveguides were lithographically patterned and ICP dry etched down to the SiO<sub>2</sub> bottom cladding layer. The etched waveguides were then capped afterward by a 2-  $\mu$  m-thick SiO<sub>2</sub> upper cladding layer to ensure better waveguide mode confinement and the reduction of propagation and scattering losses. Finally, 150-nm-thick aluminum (Al) was deposited with electron-beam evaporator and patterned via wet etch on top of the integrated device as a heating electrode.

In order to meet the design criteria as verified earlier by simulation, the refractive index contrast  $\Delta n$  of  $\sim 0.0372$  between SiO<sub>x</sub>N<sub>y</sub> core and SiO<sub>2</sub> cladding regions were chosen ( $n_{\text{SiON}} \approx 1.5082$  and  $n_{\text{SiO}_2} \approx 1.471$ ) by carefully controlling the oxygen-to-nitrogen ratio of SiO<sub>x</sub>N<sub>y</sub> during the PECVD deposition. In order to switch the optical beam intensity between the bar and cross output channels, the TO effect of SiON with a positive TO coefficient ( $\sim 2.35 \times 10^{-5}/^\circ\text{C}$ ) and a thermal conductivity of  $\sim 1.4$  W/(m•K) was applied to the lower half of the MMI multimode section by supplying the driving power to the Al heating electrode. With this bias condition asserted, the index is continuously changing and the associated magnitude change of the refractive index is expected to be graded along the x and y directions, away from the edge of the side heated region of the multimode waveguide. Therefore, we expect the maximum change in index would take place in close proximity with and also directly underneath the heating electrode while the thermal impact on the index change is expected to be faded away from the electrode.

Our device samples were first demonstrated by employing 1.55  $\mu\text{m}$  continuous-wave (cw) InGaAsP-based laser diode as a light source, a germanium (Ge) photodiode as output power detector, and a charge-coupled device (CCD) camera as a tool for observing the near-field output beam profile. The CCD (Spiricon SP-1550M) used to capture the near-field pattern is made of InGaAs and therefore it is capable of detecting the wavelength range spanning from 1460 to 1625 nm. Both the input and output ends of the optical switch were polished in order to increase the coupling efficiency. The tapered lens fiber was butt-coupled to the input facet of the device and the transmitted signal was collected with a  $\times 20$  microscope objective. The switching characteristics were obtained by applying a voltage on the heating electrode. Results were obtained and visualized with data acquisition software. As depicted Fig. 3, a cyclical switching characteristic is found; this behavior matches rather well with our earlier simulation predicted using FD-BPM shown earlier in Fig. 2. By comparing the simulation and measurement data, a few degrees shift in switching curve was most likely due to a slightly changing thermo-optic coefficient of SiON film during the actual device operation, whereas a constant thermo-optic coefficient of SiON was assumed instead in carrying out the prior FD-BPM simulation. According to the measurement data, the highest extinction coefficient found is in the excess of 13 dB.

Finally, as shown in Fig. 4, with the heating power of  $\sim 0.82$  W applied, the rise (10-90%) and fall times (90-10%) of this device were obtained as 360 and 395  $\mu\text{s}$ , respectively. The microsecond response time of thermo-optic switch is considered adequate for most types of polarization independent optical switches using dielectrics as waveguide core and cladding materials. Summarily, we believe improvements in switching power and response

speed are certainly possible through the optimizations of the overall device geometry and electrode layout, and also the adoption of different waveguide materials such as silicon-on-insulator (SOI) substrates because of their unique advantages such as higher thermal conductivity and larger thermo-optic coefficient.

The multistage MMI-based  $2 \times 2$  SiO<sub>2</sub>/SiON/SiO<sub>2</sub> optical waveguide switches were successfully designed and fabricated by employing the thermo-optic effect as working principle. Our FD-BPM simulation and subsequent device characterization results matched rather well with one another. The minor discrepancy between the simulation and experimentation data appeared to be due to a slightly changing thermo-optic coefficient of SiON film during the actual device operation, whereas a constant TO coefficient of SiON was assumed instead in carrying out the simulation. Our experimental results have demonstrated that a minimal heating power of  $\sim 0.82$  W is required to initiate the optical switching with the highest extinction coefficient in the excess of 13 dB. Finally, the temporal response measurement conducted on our devices clearly indicates the rise and fall times thereby obtained are in a neighborhood of 360 and 395  $\mu$ s, respectively. Improvements in device switching power and response speed are certainly possible through the optimizations of the overall device geometry and electrode layout, and also the incorporation of different waveguide materials of comparably better thermal and thermo-optical properties such as the SOI substrates.

## References

- [1] L. B. Soldano and E. C. M. Pennings, *J. Lightwave Technol.* **13**, 615 (1995).
- [2] Q. Lai, W. Hunziker, and H. Melchior, *IEEE Photon. Technol. Lett.* **10**, 681 (1998).
- [3] Y. Kawaguchi and K. Tsutsumi, *Electron. Lett.* **38**, 1701 (2002).
- [4] R. van Roijen, E. C. M. Pennings, M. J. N. Van Stalen, T. van Dongen, B. H. Verbeek, and J. M. M. van der Heijden, *Appl. Phys. Lett.* **64**, 1753 (1994).

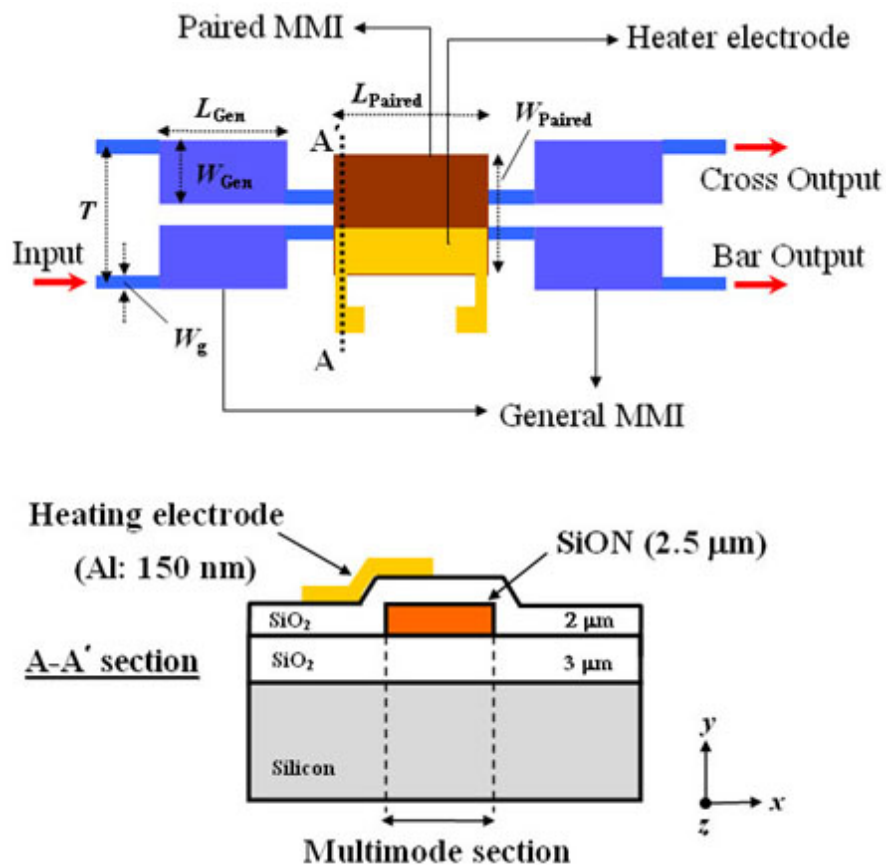


Fig. 1. Schematic drawings of cascaded  $2 \times 2$  MMI optical switch and the cross-sectional profile of the multimode

waveguide with SiON core buried in SiO<sub>2</sub> layers taken along the AA' line (not drawn to scale).

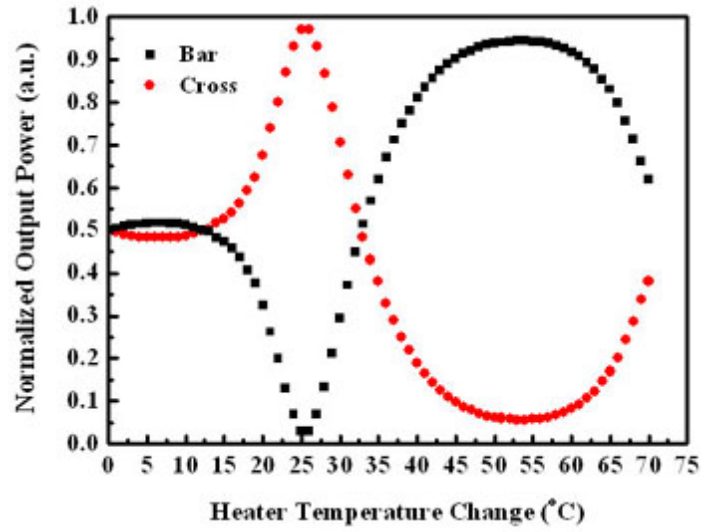


Fig. 2. The switching characteristic of a 2x2 MMI waveguide switch as simulated using the finite-difference beam propagation method (FD-BPM).

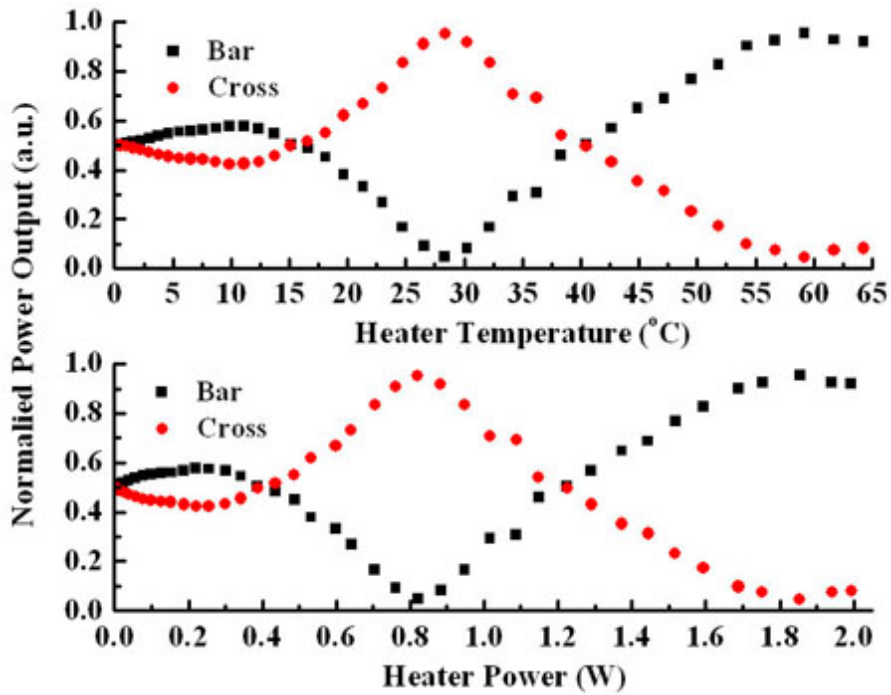


Fig. 3. The normalized power splitting ratio between bar and cross output channel of 2 x 2 MMI optical switch measured at different heating powers and also at different aluminum heater temperatures.

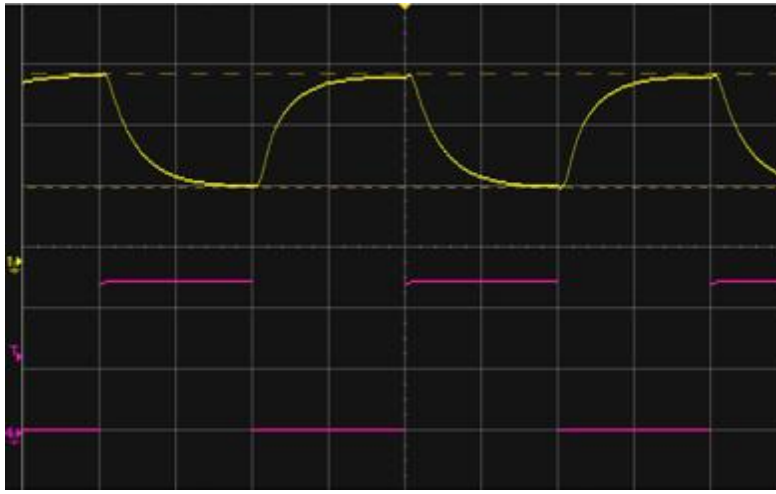


Fig. 4. Optical response (upper trace, 10 mV/div) of 2 x 2 MMI optical switch under an electrical bias switching (lower trace, 5 V/div) with a heating power of 0.82 W is applied. The horizontal time scale is set at 500  $\mu$  s/div. The rise and fall times of the switch are 360 and 395  $\mu$  s, respectively.

*Copyright 2011 National Cheng Kung University*